

## Part Orientation with a Force Field: Orienting Multiple Shapes Using a Single Field

Attawith Sudsang

Department of Computer Engineering  
Chulalongkorn University, Bangkok 10330  
Thailand

Lydia Kavraki

Department of Computer Science  
Rice University, Houston, Texas 77005  
USA

**Abstract:** *In automated assembly, before parts can be put together, they often have to be appropriately oriented and positioned. The device performing this task is generally referred to as a part feeder. A new class of devices for non-prehensile distributed manipulation, such as MEMS actuator arrays, vibrating plates, etc., provides an alternative to traditional mechanical platforms for part feeding. These devices can be abstracted as programmable vector fields. Manipulation plans for these devices can therefore be considered as strategies for applying a sequence of fields to bring parts to some desired configurations. Typically, to uniquely orient and position a part, several fields have to be sequentially employed. In our recent work [18], we have shown that this objective can be accomplished using a single field. The work characterizes such a field for a given part. In this paper, we discover another interesting property of the field. In particular, we show that for a finite set of parts (with different shapes), we can specify a single field that can uniquely orient and position every part in the set. A force field device implementing this field therefore may be used as a part feeder for every part in the set without any reconfiguration.*

## 1 Introduction

In automated assembly, before parts can be put together, they often have to be appropriately oriented and positioned. The device performing this task is generally referred to as a part feeder. The traditional and mostly used automated part feeder is the vibratory bowl feeder [8]. Vibratory bowl feeders are designed to orient a single part shape, therefore they have to be re-designed and re-built to handle different shapes. Some recent research attempts to develop systematic approaches for designing and analyzing vibratory bowl feeders [2, 13], while the mainstream research in manufacturing has focused in developing more flexible and more robust platforms, such as programmable part feeders. This type of part feeder can be programmed to handle different parts without the need for hardware modification [9, 12, 10, 1, 7].

A new direction in programmable part feeding that has recently gained attention in research is the use of a new class of devices for non-prehensile distributed manipulation. Examples are, in microscale, the use of MEMS actuator arrays [4], and in macroscale, the use of mechanical devices [15], vibrating plates [7], or air jets actuators [3]. The analysis of the capabilities of these devices is based on the abstraction of these devices as programmable vector fields. This analytical approach is pioneered by [4], where programmable vector fields are used to represent MEMS actuator array. The underlying idea is that a part lying in a force field is driven toward a stable equilibrium by the resultant force and torque induced by the field at the planar contact. This basic idea allows a manipulation task to be considered as a strategy for applying a sequence of fields to bring a part from one equilibrium to another until it reaches a desired configuration. In [4], it has been shown that polygonal parts can be oriented by a sequence of squeeze fields. The sequence is planned using an algorithm similar to the one in [12] for orienting polygonal parts with a sensorless parallel jaw gripper. The number of steps in the sequence depends on the complexity of the geometry of the convex hull of the oriented part and the uniqueness of the final orientation is only upto modulo  $180^\circ$ .

Another research direction attempting to apply force fields to the positioning problem aims at inventing a single force field that can induce a unique stable equilibrium for any part, and therefore may be used as a universal part feeder. Such a field would be able to orient any part in one step without any sensor or any sequencing control. Along this avenue, the elliptical force field that induces two stable equilibria was introduced in [14]. Further progress was presented recently in [6] with a proof confirming the conjecture in [4], namely, that there exists a combination of the unit radial field and a small constant field capable of uniquely orienting and positioning parts. The proof is based on characterization of local minima of the lifted potential function induced by the field. Unfortunately, due to the nature of the proof, this work cannot address how to compute a finite magnitude of the small constant field that

satisfies the proof. Therefore it is impossible to explicitly specify the field for a given part.

Recently, we introduced a force field that can be set to induce a unique stable equilibrium for almost any part with uniform support [18]. This force field is a combination of a linear radial force field and a constant force field. A linear radial force field is simply a radial force field for which the magnitude of the force at a point is a linear function of the distance from the point to the center of the field. The field is defined by the parameters consisting of the magnitude of the constant force field and the coefficients defining the linear function associated with the linear radial force field. Unlike [6], we showed how to explicitly determine the parameters of the field for a given part such that the part has a unique stable equilibrium when it is placed in this parameterized field. The objective of this paper is to present an important property of the field. In [18], the field is determined for a single given part. Here, we will show that, for a set of parts with different shapes, we can specify a single field such that any part in the set can be uniquely oriented. This means that, when we know the shapes of all parts under consideration, we can set a single field to orient them all without reconfiguring the field specifically for each part.

The rest of the paper is organized as follows. We will begin by giving some background and necessary notations in Section 2. In Section 3, some properties of constant fields and linear radial force fields which are the foundation of the work will be presented. Then, in Section 4, we will summarize the main contribution of our previous work for which this paper is based on, namely, the lemma specifying a field for orienting a given part. Then, in Section 5, we will present Lemma 5 which we will refer to as the main result. This lemma states how to specify a single field for orienting a set of parts with different shapes. We will then conclude the paper with some discussion in Section 6.

## 2 Background

We consider a two dimensional part with a uniform mass and area  $A$  that is placed in the plane of a force field. We attach the world frame  $(\xi, \eta)$  to this plane.

The part is in equilibrium under the field  $\mathbf{g}(\xi, \eta)$  when the resultant force  $\mathbf{F}$  and torque  $\mathbf{M}$  vanish. More precisely, an *equilibrium* is achieved if and only if

$$\mathbf{F} = \int \int \mathbf{g}(\xi, \eta) d\xi d\eta = 0 \quad \text{and}$$

$$\mathbf{M} = \int \int \begin{pmatrix} \xi \\ \eta \end{pmatrix} \times \mathbf{g}(\xi, \eta) d\xi d\eta = 0,$$

where both integrations are performed over the plane region occupied by the part. Note that the lateral force modeling used here results in first order dynamics of the motion of parts under force fields. It is a commonly used hypothesis in part orientation with force fields [5, 4, 14].

In this paper, we deal with only two types of force fields: constant fields and radial fields. A *constant field* is a force field (see Figure 1(a)) with the same force at every point and a *radial field* (see Figure 1(b)) is a force field for which all forces point toward a single center and the magnitude of the force at a point depends only on the distance between the point and the center. It is clear from the definition above that the resultant force induced by a radial field must pass through the center of the field.

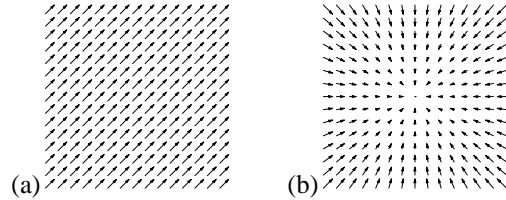


Figure 1: Examples of (a) a constant field, and (b) a radial field.

We denote by a tuple  $\langle \mathbf{c}, f(\lambda) \rangle$  a radial field with center  $\mathbf{c}$  and the force at any point  $\mathbf{p}$  be the unit force in the direction from  $\mathbf{p}$  to  $\mathbf{c}$ , scaled by  $f(\lambda)$  where  $\lambda$  is the distance between  $\mathbf{p}$  and  $\mathbf{c}$ . Note that a linear radial field is a radial field for which the function  $f$  is linear in  $\lambda$ . We also use a pictorial representation to illustrate a radial field. Figure 2 shows an example.

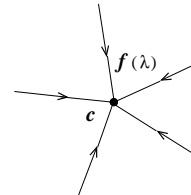


Figure 2: Pictorial representation of the radial field  $\langle \mathbf{c}, f(\lambda) \rangle$ , with  $f(\lambda) \geq 0$ . The arrows on the rays depict the direction of the forces.

We define the *pivot point*<sup>1</sup> of a part under a radial field to be a fixed point in the part's coordinate frame situated at the center of the field when an equilibrium is achieved. Note that the pivot point is unique for the unit and linear radial fields [18].

<sup>1</sup>We borrow this term from [4] where it is defined only for the unit radial field.

### 3 Geometry of Force Fields

As mentioned earlier, our force field is a combination of a linear radial field and a constant field. This section summarizes some properties of these two types of fields that are relevant to the work in this paper. Instead of purely analyzing the fields algebraically, we seek geometric explanations. As we will see soon, this approach nicely yields intuitive insight about the fields.

The following two lemmas express the relationship between the resultant forces induced by the fields and the vectors from the pivot points to the centers of the fields. This geometric relationship is very helpful as we can use it to visualize the effect of the fields on a part at different configurations. Both lemmas are thoroughly used in the proof of the main result.

**Lemma 1** For the resultant force  $\mathbf{F}$  induced by the radial field  $\mathcal{J} \stackrel{\text{def}}{=} \langle \mathbf{o}, h + k\lambda \rangle$  on a part, it is true that  $\mathbf{F} \cdot \vec{p\mathbf{o}} \geq 0$  and  $|\mathbf{F}| \geq k|\mathbf{p\mathbf{o}}|A$ , where constants  $h, k > 0$  and  $\mathbf{p}$  denote the position of the pivot point of the part under the field  $\mathcal{J}$  (Figure 3).

The proof of this lemma can be found in Appendix of the paper.

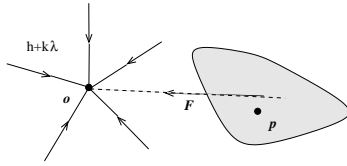


Figure 3: The resultant force  $\mathbf{F}$  induced by the radial field  $\langle \mathbf{o}, h + k\lambda \rangle$ .

**Lemma 2** The resultant force induced by the radial field  $\langle \mathbf{o}, k\lambda \rangle$  on a part is  $k\vec{p\mathbf{o}}A$ , where  $\mathbf{p}$  denotes the position of the centroid of the part (Figure 4).

The proof of this lemma is very similar to that of Lemma 1, so it is omitted here.

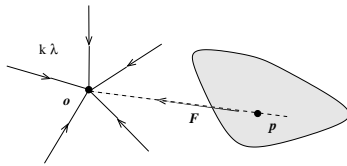


Figure 4: The resultant force  $\mathbf{F}$  induced by the radial field  $\langle \mathbf{o}, k\lambda \rangle$ .

### 4 Positioning and Orienting a Single Shape

This paper is based on the previous work which can be captured in the following lemma. In specific, the lemma shows, for a given part, how to specify a force field that induces a unique stable equilibrium for the part. The field can then be used to orient the part based on the basic idea that a part lying in a force field is driven toward a stable equilibrium configuration by the resultant force and torque induced by the field at the planar contact. Due to the space limitation, we cannot include the entire proof here. Interested readers are referred to [18]. The key idea of the proof consists of two steps. The first step identifies all possible equilibria configuration using certain properties of the fields. This step uses geometric reasoning to characterize that there are only two possible equilibrium configurations. Then second step applies potential field concept to conclude that only one configuration is stable.

**Lemma 3** Let  $h, k$  and  $c$  be arbitrary positive constants, and let  $d$  be the distance between the centroid and the pivot point of a part under the radial field  $\mathcal{K} \stackrel{\text{def}}{=} \langle \mathbf{o}, h + (k + c)\lambda \rangle$ . If  $d > 0$ , then the part has a unique stable equilibrium configuration under the combination of the radial field  $\mathcal{J}^* \stackrel{\text{def}}{=} \langle \mathbf{o}, h + (2k + c)\lambda \rangle$  and the constant field  $\mathcal{C}^* \stackrel{\text{def}}{=} \begin{pmatrix} -kd \\ 0 \end{pmatrix}$ . This stable equilibrium occurs when the part is in the configuration such that its pivot point under  $\mathcal{K}$  is positioned at  $\mathbf{o}$  and its centroid is positioned at  $\mathbf{o} - \begin{pmatrix} d \\ 0 \end{pmatrix}$ .

Note that determining the distance  $d$  for a given part requires the computation of the part's centroid and the part's pivot point under the radial field  $\mathcal{K}$ . Because the centroid of a part is essentially the center of the distribution of the part's area, it can therefore be computed, in general, using a numerical integration method [16]. The pivot point can be computed using a numerical optimization of the corresponding potential function. We present in detail in [17] a variation of this optimization approach for computing the pivot point under the linear radial  $\mathcal{K}$ .

### 5 A Single Field for Positioning and Orienting Multiple Shapes

In most works about part feeding, a strategy for part orientation is usually computed for a single part's shape. In this section, we present a rather different approach. We will show that a single field may be used to orient several parts with different shapes. A device implementing this field may be used as a part feeder for several types of parts

without any reconfiguration, resulting in more flexibility in manufacturing lines.

The result in this section is an extension of the field presented in the previous section. More precisely, in the following lemma, for a given set of parts with different shapes ( $B_i, i = 1, 2, \dots, n$ ), we will show how to set the field in Lemma 3 so that it induces a unique stable equilibrium for every part in the set. The proof of the lemma applies continuity and a monotonicity property of the field which will be given later in Lemma 5 to reduce the proof to Lemma 3.

**Lemma 4** Consider parts  $B_i, i = 1, 2, \dots, n$ , each of which has distinct shape. Let  $h, k$  and  $c$  be arbitrary positive constants and let  $d_i$  be the distance between the centroid of  $B_i$  and the pivot point of  $B_i$  under the field  $\hat{K} \stackrel{\text{def}}{=} \langle \mathbf{o}, h + (k+c)\lambda \rangle$ . Any part  $B_i, i \in \{1, 2, \dots, n\}$  with  $d_i > 0$  has a unique stable equilibrium under the combination of the radial field  $\hat{J} \stackrel{\text{def}}{=} \langle \mathbf{o}, h + (2k+c)\lambda \rangle$  and the constant field  $\hat{C} \stackrel{\text{def}}{=} \begin{pmatrix} -kd^* \\ 0 \end{pmatrix}$ , where  $d^* = \min\{d_i, i = 1, 2, \dots, n\}$ .

PROOF: Consider the part  $B_j, j \in \{1, 2, \dots, n\}$ . If  $d_j = d^*$ , the lemma follows immediately from Lemma 3. For the case  $d_j > d^*$ , let us denote by  $d'_j$  the distance between the centroid of  $B_j$  and the pivot point of  $B_j$  under the radial field  $\langle \mathbf{o}, h + (2k + c - k_j)\lambda \rangle$ . By definition, we have  $d'_j = d_j$  when  $k_j = k$  and consequentially  $k_j d'_j > kd^*$ . Using Lemma 5, as the value of  $k_j$  decreases, the value of  $d'_j$  decreases monotonically. By continuity, this implies that there exists a value  $k_j = k_j^* \in (0, k)$  and corresponding  $d'_j = d_j^* < d_j$  for which  $k_j^* d_j^* = kd^*$ . We can therefore rewrite  $\hat{C} \stackrel{\text{def}}{=} \begin{pmatrix} -kd^* \\ 0 \end{pmatrix} = \begin{pmatrix} -k_j^* d_j^* \\ 0 \end{pmatrix}$  and  $\hat{J} \stackrel{\text{def}}{=} \langle \mathbf{o}, h + (2k + c)\lambda \rangle = \langle \mathbf{o}, h + (2k_j^* + c')\lambda \rangle$  where  $c' = 2k + c - 2k_j^*$ . Because  $k_j^* \in (0, k)$ , we have  $c' > 0$  and once again the lemma follows from Lemma 3. ■

From Lemma 4, computing the field  $\hat{J}$  and  $\hat{C}$  amounts to computing all  $d_j$ 's. This requires the computation of the pivot point of each  $B_j$  under the field  $\hat{K}$ . As mentioned in the previous section, pivot point computation is discussed in detail in [18]. The computation of the stable equilibrium of each  $B_j$  can be found by considering Lemma 3 with the rewritten fields  $\hat{J} \stackrel{\text{def}}{=} \langle \mathbf{o}, h + (2k_j^* + c')\lambda \rangle$  and  $\hat{C} \stackrel{\text{def}}{=} \begin{pmatrix} -k_j^* d_j^* \\ 0 \end{pmatrix}$  which are given near the end of the proof of Lemma 4. This computation requires us to seek the value of  $k_j$  for which  $k_j d'_j = kd^*$ . Since  $d'_j$  can be considered as a monotonic function of  $k_j$ , the search can be performed using the bisection method on the range  $(0, k)$ .

The following lemma helps complete the proof of Lemma 4. The lemma identifies that the distance between the centroid and the pivot point under a linear radial field is a monotonic function of the linear coefficient of the field.

**Lemma 5** Let  $d_1 = |P_1 P|$  and  $d_2 = |P_2 P|$  where  $P$  is the centroid, of a part, and  $P_1$  and  $P_2$  are the pivot points of the same part under the radial fields  $\mathcal{J}_1 = \langle \mathbf{o}, h + k_1\lambda \rangle$  and  $\mathcal{J}_2 = \langle \mathbf{o}, h + k_2\lambda \rangle$  respectively. For constants  $h, k_1, k_2 > 0$  and  $P_1 \neq P$ , if  $k_2 > k_1$ , we have  $d_2 < d_1$ .

PROOF: Let us denote by  $\mathbf{p}, \mathbf{p}_1$  and  $\mathbf{p}_2$  the positions of  $P, P_1$  and  $P_2$  in the world frame. Let us suppose that the part is now at a configuration  $\mathbf{q}$  where it is in equilibrium under the field  $\mathcal{J}_1$ . This implies that  $\mathbf{p}_1 = \mathbf{o}$  when the part is at this configuration  $\mathbf{q}$ . Imagine that we add to the system the radial field  $\mathcal{J}_2' \stackrel{\text{def}}{=} \langle \mathbf{o}, kr \rangle$  where  $k = k_2 - k_1 > 0$ . By Lemma 2 and the fact that  $P \neq P_1$ , the part can no longer be in equilibrium at the configuration  $\mathbf{q}$  under the combination of the radial fields  $\mathcal{J}_1$  and  $\mathcal{J}_2'$ . Let us consider the part under this combination of the fields at another configuration: in particular, consider an arbitrary configuration for which  $\overrightarrow{\mathbf{p}\mathcal{O}} \cdot \overrightarrow{\mathbf{p}_1\mathcal{O}} > 0$ . From Lemma 2, we have  $\mathbf{F}_2 = k\overrightarrow{\mathbf{p}\mathcal{O}}$  where  $\mathbf{F}_2$  is the force induced by the field  $\mathcal{J}_2'$  and from Lemma 1, we have  $\mathbf{F}_1 \cdot \overrightarrow{\mathbf{p}_1\mathcal{O}} > 0$  where  $\mathbf{F}_1$  is the force induced by the field  $\mathcal{J}_1$ . But  $\overrightarrow{\mathbf{p}\mathcal{O}} \cdot \overrightarrow{\mathbf{p}_1\mathcal{O}} > 0$  implies that  $\mathbf{F}_2 \cdot \overrightarrow{\mathbf{p}_1\mathcal{O}} > 0$  and consequentially that an equilibrium is impossible because  $(\mathbf{F}_1 + \mathbf{F}_2) \cdot \overrightarrow{\mathbf{p}_1\mathcal{O}} > 0$ . This means that an equilibrium under  $\mathcal{J}_1 + \mathcal{J}_2'$  can be achieved only when  $\overrightarrow{\mathbf{p}\mathcal{O}} \cdot \overrightarrow{\mathbf{p}_1\mathcal{O}} \leq 0$  (a necessary condition).

It is easy to verify that when  $\overrightarrow{\mathbf{p}\mathcal{O}} \cdot \overrightarrow{\mathbf{p}_1\mathcal{O}} \leq 0$ , we always have  $|\mathbf{p}\mathcal{O}| < |\mathbf{p}_1\mathcal{P}|$  (Figure 5). Because the combination of  $\mathcal{J}_1$  and  $\mathcal{J}_2'$  is essentially  $\mathcal{J}_2$ , we therefore know that  $\mathbf{p}_2 = \mathbf{o}$  when the object is in equilibrium. We can thus write  $d_2 = |P_2 P| = |\mathbf{o}\mathbf{p}|$ . Recall that  $d_1 = |P_1 P| = |\mathbf{p}_1\mathbf{p}|$ . We therefore have  $d_2 < d_1$  and complete the proof. ■

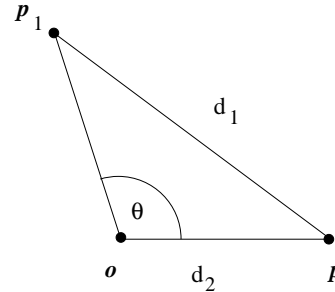


Figure 5: When  $\overrightarrow{\mathbf{p}\mathcal{O}} \cdot \overrightarrow{\mathbf{p}_1\mathcal{O}} \leq 0$ , we have  $\theta \in [\frac{\pi}{2}, \pi]$  and  $|\mathbf{p}\mathcal{O}| < |\mathbf{p}_1\mathcal{P}|$ .

We have shown how to set a force field for orienting a set of parts with different shapes. Besides part feeding, an interesting application of this field is part sorting. One

idea is to combine a force field device with physical separators, such as fences above the plane of force field. For instance, two parts with different shapes can be sorted as follows. First, we set the field to orient both parts according to Lemma 4. Place an input part on this field to bring it to a unique equilibrium. Then reprogram the field to behave as a conveyer belt to move the part through separating fences. Because we can compute the unique equilibrium for each part under the field (Lemma 4) and we can design a sequence of fences and traps that let go only a specific part's shape at a certain orientation [19], we therefore can build a sorter system that allow only one type of part to pass. More complex sortor may also be built using this basic.

## 6 Discussion and Conclusion

The use of force fields as a modeling tool for analyzing hardware force field devices has become a common practice because it usually leads to tractable analytical results. Although this modeling approach is reasonable, it does not address the discretization which is usually inherent in most hardware implementation. This calls for a careful investigation on the effect of discretization.

In this paper, we have presented a way to program a force field for orienting a set of parts with different shapes. Being able to bring a part from an unknown configuration to a known one is an elimination in the part's configuration uncertainty. Being able to do as such for several types of parts may also be considered as some sort of tolerance for uncertainty in part's geometry. However, in our method, geometry of a part is captured in terms of the distance between the part's pivot point and its centroid. Therefore, our next goal is to study analytical relationship between the distance and the geometry. This knowledge would ultimately help us describe variation of part's shapes that could be oriented by a given field.

## Appendix

### Proof of Lemma 1

Without loss of generality, let us assume that  $\mathbf{o} = \begin{pmatrix} 0 \\ 0 \end{pmatrix}$ , and rewrite the field  $\mathcal{J}$  as the combination of two radial fields  $\mathcal{J}_1 \stackrel{\text{def}}{=} \langle \mathbf{o}, k\lambda \rangle$  and  $\mathcal{J}_2 \stackrel{\text{def}}{=} \langle \mathbf{o}, h \rangle$ . Let us denote by  $\mathbf{f}_1, \mathbf{f}_2 : \mathbb{R}^2 \mapsto \mathbb{R}^2$  the functions that map point positions in the world frame to the forces at the positions induced by  $\mathcal{J}_1$  and  $\mathcal{J}_2$  correspondingly. Also, let us denote by  $P$  the pivot point under  $\mathcal{J}$  and by  $M$  an arbitrary point of the part. Let  $\mathbf{p}$  and  $\mathbf{m} = \begin{pmatrix} \xi \\ \eta \end{pmatrix}$  denote the positions of

$P$  and  $M$  in the world frame when the part is at a configuration  $\mathbf{q}$ .

By setting  $\mathbf{g}_i(\mathbf{m}) = \mathbf{f}_i(\mathbf{m}) - \mathbf{f}_i(\mathbf{m} - \mathbf{p})$ , for  $i = 1, 2$ , we can write the resultant force at  $\mathbf{m}$  as  $\mathbf{f}(\mathbf{m}) = \mathbf{f}_1(\mathbf{m}) + \mathbf{f}_2(\mathbf{m}) = \mathbf{f}_1(\mathbf{m} - \mathbf{p}) + \mathbf{f}_2(\mathbf{m} - \mathbf{p}) + \mathbf{g}_1(\mathbf{m}) + \mathbf{g}_2(\mathbf{m})$  and we can write the resultant force  $\mathbf{F}$  exerted on the part at the configuration  $\mathbf{q}$  as

$$\begin{aligned} \iint \mathbf{f}_1(\mathbf{m}) + \mathbf{f}_2(\mathbf{m}) d\xi d\eta = \\ \iint \mathbf{f}_1(\mathbf{m} - \mathbf{p}) + \mathbf{f}_2(\mathbf{m} - \mathbf{p}) d\xi d\eta + \\ \iint \mathbf{g}_1(\mathbf{m}) d\xi d\eta + \\ \iint \mathbf{g}_2(\mathbf{m}) d\xi d\eta, \end{aligned} \quad (1)$$

with all the integrations performed over the plane region occupied by the part at the configuration  $\mathbf{q}$ . It is easy to see that the first term of the right side of Equation 1 vanishes. This is because  $\mathbf{f}_1(\mathbf{m} - \mathbf{p}) + \mathbf{f}_2(\mathbf{m} - \mathbf{p})$  is essentially the force at the point  $M$  when the part is at the configuration such that the pivot point  $P$  is positioned at the field's center  $\mathbf{o}$  and the orientation of the part is the same as that of the configuration  $\mathbf{q}$ . We therefore need to consider only the second and the third terms.

Consider the second term of the right side of Equation 1. From the definition, we have  $\mathbf{g}_1(\mathbf{m}) = \mathbf{f}_1(\mathbf{m}) - \mathbf{f}_1(\mathbf{m} - \mathbf{p}) = (-k\mathbf{m}) - (-k(\mathbf{m} - \mathbf{p})) = -k\mathbf{p} = k\vec{\mathbf{p}\mathbf{o}}$ . As a result, we obtain  $\iint \mathbf{g}_1(\mathbf{m}) d\xi d\eta = k\vec{\mathbf{p}\mathbf{o}}A$ .

Now consider the third term of the right side of Equation 1. Let  $a = |\mathbf{p}\mathbf{m}|$ ,  $b = |\mathbf{o}\mathbf{m}|$ ,  $\alpha = \angle \mathbf{p}\mathbf{m}\mathbf{o}$ , and  $\phi$  be the angle between  $\vec{\mathbf{m}\mathbf{p}}$  and the x-axis (Figure 6). We can write

$$\begin{aligned} \mathbf{f}_2(\mathbf{m}) &= h \begin{pmatrix} \cos(\phi + \alpha) \\ \sin(\phi + \alpha) \end{pmatrix}, \\ \mathbf{f}_2(\mathbf{m} - \mathbf{p}) &= h \begin{pmatrix} \cos \phi \\ \sin \phi \end{pmatrix}, \\ \mathbf{p} &= \mathbf{m} + a \begin{pmatrix} \cos \phi \\ \sin \phi \end{pmatrix} \quad \text{and} \\ \mathbf{o} &= \mathbf{m} + b \begin{pmatrix} \cos(\phi + \alpha) \\ \sin(\phi + \alpha) \end{pmatrix}. \end{aligned}$$

We thus obtain after some simplification

$$\mathbf{g}_2(\mathbf{m}) \cdot \vec{\mathbf{p}\mathbf{o}} = h(a + b)(1 - \cos \alpha),$$

which implies

$$\left( \iint \mathbf{g}_2(\mathbf{m}) d\xi d\eta \right) \cdot \vec{\mathbf{p}\mathbf{o}} \geq 0.$$

As a result, we have

$$|\mathbf{F}| \geq \left| \iint \mathbf{g}_1(\mathbf{m}) d\xi d\eta \right| = k|\mathbf{p}\mathbf{o}|A, \quad \text{and}$$

$$\mathbf{F} \cdot \vec{\mathbf{p}\mathbf{o}} = \left( \iint \mathbf{g}_1(\mathbf{m}) + \mathbf{g}_2(\mathbf{m}) d\xi d\eta \right) \cdot \vec{\mathbf{p}\mathbf{o}} \geq 0. \quad \blacksquare$$

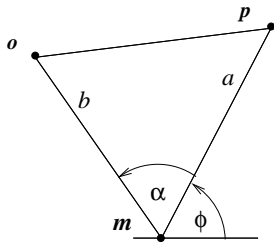


Figure 6: Arrangement of point  $M$  with respect to the pivot point and the center.

## Acknowledgements

Work on this paper by Attawith Sudsang and Lydia Kavraki has been supported in part by NSF IRI-970228, NSF CISE SA1728-21122N and a Sloan Fellowship to Lydia Kavraki.

## References

- [1] S. Akella, W. Huang, K. Lynch, and M. Mason. Sensorless parts orienting with a one-joint manipulator. In *IEEE Int. Conf. on Robotics and Automation (ICRA)*, pages 2383–2390, Albuquerque, NM, April 1997.
- [2] D. Berkowitz and J. Canny. Designing parts feeders using dynamic simulation. In *Proc. IEEE Int. Conf. Robotics and Automation*, Minneapolis, MN, 1996.
- [3] D. Biegelsen, W. Jackson, A. Berlin, and P. Cheung. Air jet arrays for precision positional control of flexible media. In *Proc. Int. Conf. on Micromechatronics for Information and Precision Equipment*, pages 631–634, Tokyo, Japan, 1997.
- [4] K.-F. Böhringer, B. Donald, and N. MacDonald. Upper and lower bounds for programmable vector fields with applications to MEMS and vibratory plate parts feeders. In Jean-Paul Laumond and Mark Overmars, editors, *Algorithms for Robotic Motion and Manipulation*, pages 255–276. A. K. Peters, Ltd, Wellesley, MA 02181, 1997.
- [5] K.-F. Böhringer, B. R. Donald, R. Mihailovich, and N. C. MacDonald. Sensorless manipulation using massively parallel microfabricated actuator arrays. In *IEEE Int. Conf. on Robotics and Automation*, pages 826–833, 1994. San Diego, CA.
- [6] K.-F. Böhringer, B. R. Donald, L. Kavraki, and F. Lamiraux. Part orientation with one or two stable equilibria using programmable vector fields. *IEEE Transactions on Robotics and Automation*, 16(2), 2000, pages 157–170.
- [7] K.-F. Böhringer, V. Bhatt, and K.Y. Goldberg. Sensorless manipulation using transverse vibrations of a plate. In *Proc. IEEE Int. Conf. on Rob. and Autom.*, pages 1989–1996, 1995.
- [8] G. Boothroyd, C. Poli, and L. Murch. *Automatic Assembly*. Marcel Dekker, Inc., 1982.
- [9] Y.B. Chen and D.J. Ierardi. The complexity of oblivious plans for orienting and distinguishing polygonal parts. *Algorithmica*, 14:367–397, 1995.
- [10] M. Erdmann and M. Mason. An exploration of sensorless manipulation. *IEEE Tr. on Rob. and Autom.*, 4(4):369–379, 1988.
- [11] F. Lamiraux and L. Kavraki. Positioning and Orienting Symmetric and Non-Symmetric Parts Using a Combination of a Unit Radial and Constant Force Fields. *International Workshop on the Algorithmic Foundation of Robotics*, TH28-TH42, March, 2000.
- [12] K. Y. Goldberg. Orienting polygonal parts without sensors. *Algorithmica*, 10:201–225, 1993.
- [13] M. Jakiela and J. Krishnasamy. Computer simulation of vibratory parts feeding and assembly. In *Proc. 2nd Int. Conf. Discrete Element Methods*, 1993.
- [14] L. E. Kavraki. Part orientation with programmable vector fields: Two stable equilibria for most parts. In *Proc. IEEE Int. Conf. on Robotics and Automation*, pages 2446–2451, 1997.
- [15] J. Luntz, W. Messner, and H. Choset. Velocity field design for parcel manipulation on the virtual vehicle, a discrete distributed actuator array. In P.K. Agarwal, L. E. Kavraki, and M. Mason, editors, *Robotics: The Algorithmic Perspective*, pages 35–47. AK Peters, Natick, MA, 1998.
- [16] Ahmed A. Shabana. *Computational Dynamics*. John Wiley & Sons, New York, 1994.
- [17] A. Sudsang and L. Kavraki. *A force field for orienting and positioning parts in the plane*. Submitted to *IEEE Tr. on Rob. and Autom.*
- [18] A. Sudsang and L. Kavraki. *A Geometric approach to designing a programmable force field with a unique stable equilibrium for parts in the plane*. In *Proc. IEEE Int. Conf. on Robotics and Automation*, 2001.
- [19] J. Wiegley and K. Goldberg and M. Peshkin and M. Brokowski. *A Complete Algorithm for Designing Passive Fences to Orient Parts*. In *Proc. IEEE Int. Conf. on Robotics and Automation*, 1996